Mattheus, W. & Brücker, C. (2011). Asymmetric glottal jet deflection: differences of two- and three-dimensional models. The Journal of the Acoustical Society of America (JASA), 130(6), EL373 -EL379. doi: 10.1121/1.3655893

CITY UNIVERSITY LONDON

EST 1894

City Research Online

Asymmetric glottal jet deflection: Differences of two- and three-dimensional models

Willy Mattheus[a)] and Christoph Brücker
*Department of Mechanics and Fluid Dynamics, TU Bergakademie Freiberg,
Lampadiusstrasse 4, 09599 Freiberg, Germany
willy.mattheus@imfd.tu-freiberg.de, bruecker@imfd.tu-freiberg.de*

Abstract: Flow is studied through a channel with an oscillating orifice mimicking the motion of the glottal-gap during phonation. Simulations with prescribed flow and wall-motion are carried out for different orifice geometries, a 2D slit-like and a 3D lens-like one. Although the jet emerges from a symmetric orifice a significant deflection occurs in case of the slit-like geometry, contrary to the 3D lens-like one. The results demonstrate the dependency of jet entrainment and vortex dynamics on the orifice geometry and the interpretation of asymmetric jet deflection with regard to the relevance of the Coanda effect in the process of human phonation.

1. Introduction

The stability and penetration path of jet-like flows into enclosed cavities are largely influenced by the presence of the nearby sidewalls (Reynolds *et al.*[1]). In addition, when the jet-like flow is modulated in time the situation may even become more complex, since different time-scales of the flow such as the jet build-up time and the characteristic turn-over time of fluid captured in recirculation regions are both involved in the process. In principle, such a situation is produced by the flow-induced oscillatory motion of the vocal folds during human phonation, which leads to a pulsating jet-like flow penetrating into the cavity downstream of the glottis.

In a recent study Zheng *et al.*[2] investigated the jet deflection by a 2D numerical simulation of the glottal constriction in the case of constant glottal opening angle. They state that the large scale asymmetry of the flow downstream of the constriction is mainly influencing the jet deflection. The direction of jet deflection can be altering from cycle to cycle while the angle of glottal opening is not that important. Erath and Plesniak[3] also agree with this statement by experimental investigation of the flow in a scaled up vocal folds model with rectangular slit-like orifice.

As a contribution to this discussion we did a series of numerical two- and three-dimensional computations of the incompressible flow through a glottal like constriction. Especially the three-dimensional computations are an extension to the presented models in literature by now. The simulations are applied to a 3D geometrical model of the human glottis with moving walls, which has already been published in literature and was used for extensive experimental flow studies, see Triep and Brücker[4] and Triep *et al.*[5] This model reproduces the glottal motion with a lens-like elliptic shape of the orifice, as observed in clinical studies for healthy phonation by Inwald *et al.*[6] The results are compared to more simplified slit like models often used in numerical and experimental studies published by now. The behavior of the emerging jet shows significant differences between the 2D computation, the 3D computation with slit-like orifice and the 3D computation with lens-like orifice.

[a)]Author to whom correspondence should be addressed.

The present letter addresses the ongoing discussion whether observations of jet deflection in simulations and model studies of the glottal flow are indicative for the presence of the Coanda effect in human phonation. The objective of the study is to demonstrate the sensitivity of the pulsating jet flow to the shape of the orifice and to underline the need for adequate models that replicate the 3D motion of the glottis in a more realistic way. The differences in the flow field between the 2D and 3D models might furthermore explain differences in the resulting acoustic spectrum.

2. Numerical methods/CFD model

The numerical model presented here has already been validated and shown to capture the jet dynamics including flow separation, shear-layer roll-up and vorticity dynamics by Schwarze et al.[7] Therefore, it is only presented shortly, and the reader is referred to the full paper for more details. The model solves for the time-dependent, incompressible Navier-Stokes equations of Newtonian fluids in three-dimensional flows. The discretized model equations are numerically solved with the finite-volume method in a cell-centered formulation on a fully block structured grid with the open source CFD code OpenFOAM.

The geometry corresponds to the experimental setup published by Triep and Brücker[4] and Triep et al.[5] It consists of a straight channel with quadratic cross-section, in which the constriction—built from two opposite facing curved walls representing the glottis with both vocal folds—is placed symmetric to the center-plane. The dimensions based on the edge length D of the squared channel cross-section are given in Fig. 1(a). The walls are modulated by rotating cams such that the gap between both walls changes over the modulation cycle from a fully opened orifice to a fully closed orifice and vice versa. This wall movement reproduces the convergent-divergent opening/closing transition of the glottal gap contour during the phonation cycle as reported by Hirano.[8] For all simulations, the glottal contour remains 50% of the total cycle time in closed position which represents an open quotient of 50%. The importance of flow
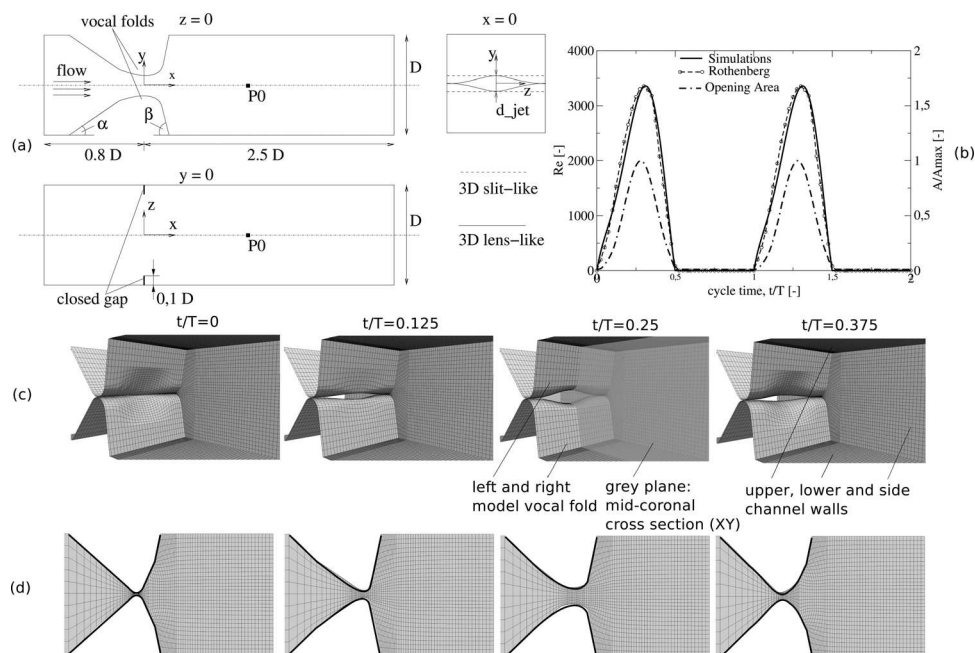

Fig. 1. (a) Dimensions of the computational regime. (b) Prescribed glottal waveform, synchronous to the opening and closure of the constriction. (c) Surface contours for 4 successive time-steps. (d) Contours in the mid-coronal cross section.

separation phenomena in glottal flows is shown by Alipour et al.[9] In the presented study the near wall region has been refined to a dimensionless wall distance of $y^+ \approx 1$.

The pulsating flow is generated by a periodic waveform function of the volume flow rate, see Fig. 1(b), which is prescribed at the inflow boundary synchronous in time to the periodic opening and closing of the glottal gap. This waveform is a result of measurements by Triep et al.[4] obtained with the dynamic cam model under certain trans-glottal pressure conditions. It is also in very good agreement with Rothenbergs data[10] obtained by the inverse filtering technique. During one waveform cycle the bulk fluid in the sub-glottal channel is displaced by approximately 0.1D in streamwise direction, thus the inflow into the glottal area is not disturbed by the boundary upstream of the constriction. The jet Reynolds number is defined herein with the time-dependent centerline velocity in the glottal gap and the maximum glottal gap width $D_{\max}$. The peak Reynolds number of ≈ 3350 is equal among all cases.

The no-slip condition for velocity and zero gradient condition for pressure are defined in normal direction to each wall boundary. The extension of the computational domain downstream of the glottis was varied between 2.5D, 5D to a maximum of 10D. The results did not show any significant differences in vortex dynamics. Therefore the extension of the computational domain downstream of the glottis is limited to 2.5D in the 3D simulation cases to profit from reduced computational effort and a maximum of grid resolution in the relevant region. Due to the relatively short penetration depth of the glottal jet into supra-glottal region within each cycle of only 1D to 1.5D, the outflow boundary is only charged with weak vortical structures leaving the computational domain, see visualization pictures in Fig. 2. Additionally the implemented outflow boundary condition for the pressure field, called "fixed mean value," fits the average value of the boundary to the given one. That reduces the distortion of the flow at the outflow boundary condition very much. Overall, a total number of 10 cycles were computed for each configuration (2D, 3D slit-like, 3D lens-like) on the cluster "PC-farm Deimos" installed at the high-performance computing center "ZIH Dresden."

3. Results and discussion

The results of the flow field are illustrated in Figs. 2(a)–2(c) by a scalar tracer field, that is injected at the inflow boundary condition and set to the value 1. It is transported through the flow field based on a convection-diffusion equation. The diffusion coefficient is set close to zero such that the resulting tracer distribution field represent streak surfaces or the images of classical dye-based flow visualization. Note that the figures only illustrate the tracer distribution patterns in the mid-coronal cross-section of the channel such as a laser-light sheet visualization experiment would do. This way, the penetration pattern of the pulsating jet into the downstream cavity as well as the downstream organization of recirculation regions can easily be recognized from the data of the numerical results.

For the characterization of the flow field symmetry the velocity field is evaluated along two different lines parallel to the y-axis positioned at $x/H = 0.16$; $z = 0$ and $x/H = 0.25$; $z = 0$ downstream of the jet orifice. The point of maximum jet velocity relative to the centerline is determined, which is a measure of the lateral offset of the jet core relative to the axis. Based on this offset, the angle of jet deflection is calculated similar to the procedure used in Zheng et al.[2] No interpolation is used; therefore, the uncertainty in the value of the angle is determined by the lateral grid-spacing in this region, an estimation of this uncertainty gives a value of $\pm 2°$. The results are shown as bar-type plots of the jet deflection angle over time, which resembles a spatio-temporal reconstruction of the jet-core offset location.

At both evaluated positions the tendency of the jet deflection is nearly the same in value and time; therefore, we display only the profiles for the further downstream position, see Fig. 3.
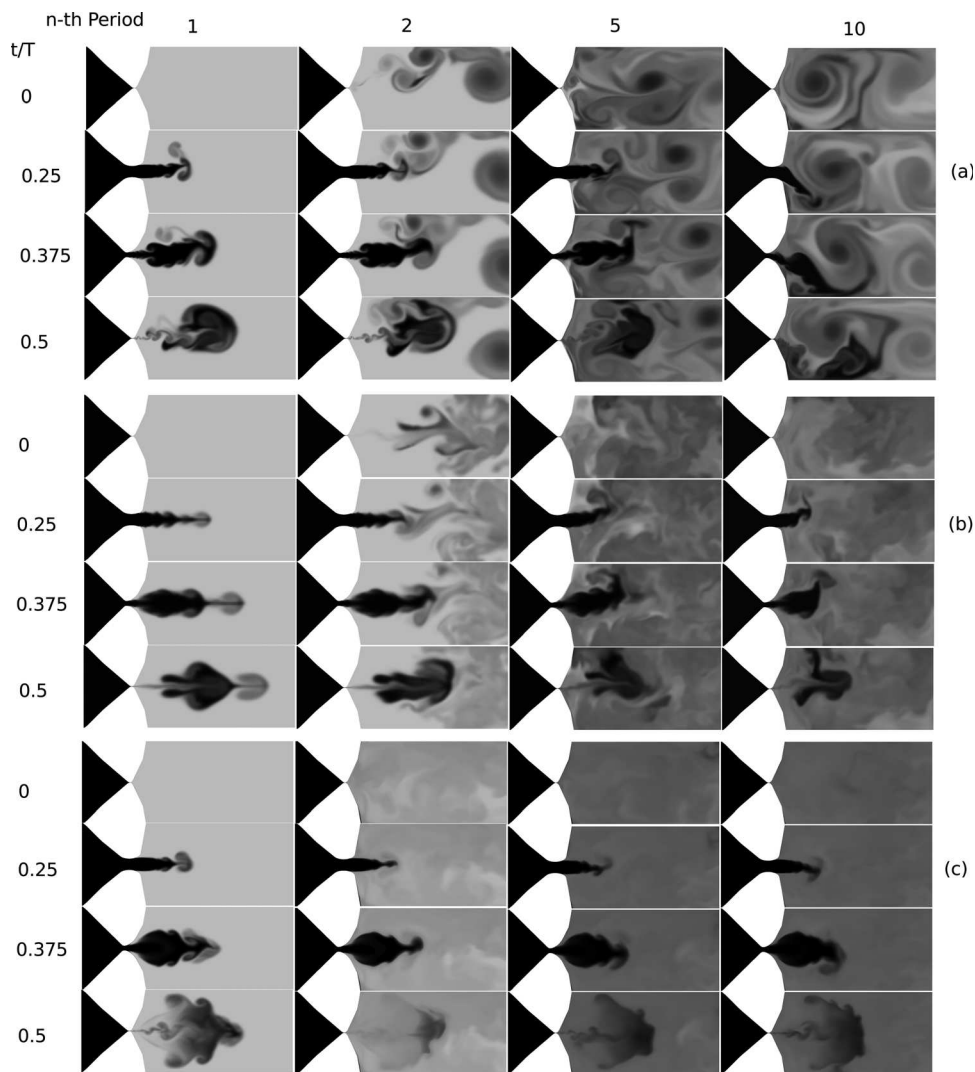
Fig. 2. Tracer field for (a) 2D computation, (b) 3D computation with slit-like orifice, and (c) 3D computation with lens-like orifice.

The 2D simulation shows strongest deflection compared to the other cases. The asymmetry of the jet already starts in the first cycle and can be clearly detected in the third cycle as a first pronounced disturbance of the jet flow with a deflection angle larger than 20 (see Fig. 3). For the 3D slit-like case the deflection angle grows from cycle to cycle up to the 5th cycle with a deflection angle of 20, and then the deflection remains nearly unchanged at high levels. Finally, for the 3D lens-like case the is no significant jet deflection observable for the simulated 10 cycles.

The effect of the closed phase of the constriction can be clearly seen in the diagrams in Fig. 3 at least for the three dimensional simulations. During the closed phase of the orifice there is no sign of remaining cross-wise flow with considerable large fluid velocity downstream of the constriction. Contrary to that, in case of the two-dimensional simulation the large eddies remain for longer times in the supra-glottal region, so that they influence especially the evaluated results along line $x/H = 0.25$. The reason is the difference of jet entrainment and vorticity dynamics in 2D and 3D flow.
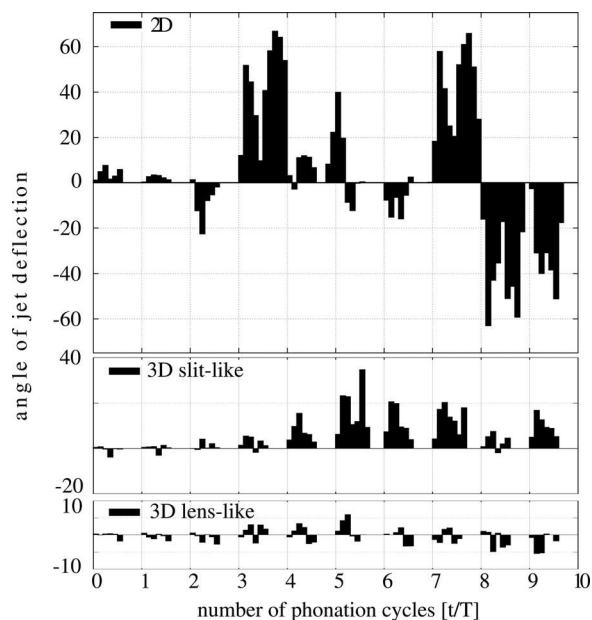
Fig. 3. Spatio-temporal reconstruction of the angle of jet deflection at position $x/H=0.25$ (uncertainty of $\pm 2°$).

A comparison of the vortex structures is presented in Fig. 4. A clear difference in the vortex core arrangement is seen for the slit-like orifice in comparison to the lens-like orifice. In the latter, the jet develops the so-called axis-switching effect, which redistributes vorticity from the spanwise component into the cross-wise and streamwise direction. In contrast, the vortex cores in the slitlike case remain nearly straight spanwise rollers with concentrated spanwise vorticity except of the very near wall region. Therefore, the jet entrainment effect and the turbulent breakdown further downstream differ largely for both cases. Finally, for the 2D simulation there is no redistribution of vorticity at all. In case of any 2D simulation, vorticity is only a scalar field. Energy
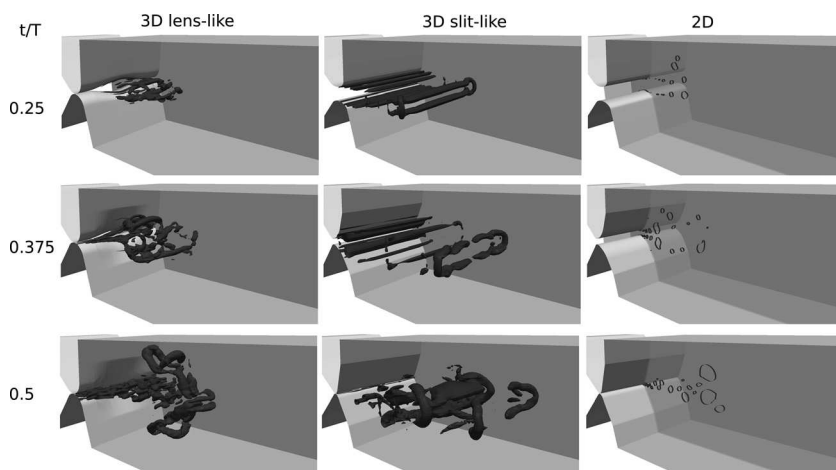

Fig. 4. Vortical structures visualized by iso-value of Q-criterion (iso-value = 2000) at certain times t/T during cycle for the simulation runs with 3D lens-like shaped constriction, 3D slit-like constriction and the 2D case, with a constriction that equals the mid-cross section (XY) of the two 3D cases.

cannot be distributed in other directions than within the flow plane, thus the entrainment effect of the jet in combination with the lateral restrictions due the channel walls leads to larger recirculation regions, which are continuously fed and sustained by the jet. Such a large supra-glottal recirculation is well seen at the 10th period in the 2D simulation.

These large scale recirculation regions occurring for slit-like configurations are continuously fed by the successive penetrating jet and do not decay as much as in the lens-like case during the closed phase of the constriction. As a consequence the persistent recirculation regions might contribute to the low frequency part of the aeroacoustic spectrum. The stronger jet deflection for the slit-like cases also induces jet-wall interaction and thereby generates additional acoustic sources.

4. Conclusion

The results of the numerical simulation of the jet dynamics in models with dynamical moving glottal gap contours and orifices show a clear dependency of the appearance of asymmetric jet deflection, whether a simplified slit-like or more realistic 3D lens-like model of the glottal orifice shape is used. For both cases the boundary conditions of the applied waveform, the symmetric opening behavior and the open quotient are the same to investigate the pulsating glottal jet flow. The only difference is the shape of the orifice. For the simplified slit-like geometry no axis-switching effect is observed. In addition, strong asymmetric jet deflection evolves after a certain number of cycles due to the generation of large recirculation regions in the supra-glottal space. In contrast, the three-dimensional effect of axis switching is clearly observed for 3D lens-like geometry. This result demonstrates the different behavior of jet entrainment for the simplified slit-like and the more complex lens-like model. The same holds for experiments with slit-like planar orifices, where the vortex dynamics in the pulsating jet flow show a clear 2D tendency during the built-up and breakdown of the jet. Since jet entrainment and vorticity dynamics differ very much in 2D and 3D models, any observation of asymmetric jet deflection in simplified models must be interpreted with caution regarding the presence of a possible Coanda effect in the process of human phonation. Rather our results show that the Coanda effect might not be a relevant flow feature in the glottal jet flow. As a consequence, 2D models may overestimate the aeroacoustic contribution of jet-wall interaction and may generate artificial low-frequency patterns in the acoustic spectrum due to the falsified generation of large recirculation region in the supra-glottal space.

Finally, it should be mentioned that such flow details are largely influenced by the supra-glottal channel geometry and the open quotient of the wave-form. Although our model geometry cannot be in all details regarded as a physical correct replication of the human phonation cycle, it, however, clearly demonstrates the shortcomings of 2D simulations or models with straight parallel contours of the vocal folds regarding the interpretation of acoustical relevant flow details.

References and links

[1] W. C. Reynolds, D. E. Parekh, P. J. D. Juvet, and M. J. D. Lee, "Bifurcating and blooming jets," Ann. Rev. Fluid Mech. **35**, 295–315 (2003).

[2] X. Zheng, R. Mittal, and S. Bielamowicz, "A computational study of asymmetric glottal jet deflection during phonation," J. Acoust. Soc. Am. **129**(4), 2133–2142 (2011).

[3] B. D. Erath and M. W. Plesniak, "Impact of wall rotation on supraglottal jet stability in voiced speech," J. Acoust. Soc. Am. **129**(3), EL64–EL70 (2011).

[4] M. Triep and C. Brücker, "Three-dimensional flow nature of the supraglottal jet," J. Acoust. Soc. Am. **127**(3), 1537–1547 (2010).

[5]M. Triep, C. Brücker, M. Stingl, and M. Döllinger, "Optimized transformation of the glottal motion into a mechanical model," Med. Eng. Phys. **33**, 210–217 (2011).

[6]E. C. Inwald, M. Döllinger, M. Schuster, U. Eysholdt, and C. Bohr, "Multiparametric analysis of vocal fold vibrations in healthy and disordered voices in high-speed imaging," J. Voice **25**, 576–590 (2011).

[7]R. Schwarze, W. Mattheus, J. Klostermann, and C. Brücker, "Starting jet flows in a three-dimensional channel with larynx-shaped constriction," Comp Fluids **48**(1), 68–83 (2011).

[8]M. Hirano, T. Yoshida, and S. Kurita, "Anatomy and behavior of the vocal process," in *Laryngeal Function in Phonation and Respiration*, edited by T. Baer, C. Sasaki, and K. Harris, (College Hill Press, Boston, 1987), pp. 1–13.

[9]F. Alipour and R. C. Scherer, "Flow separation in a computational oscillating vocal fold model," J. Acoust. Soc. Am. **116**, 1710–1719 (2004).

[10]M. Rothenberg, "A new inverse-filtering technique for deriving the glottal airflow waveform during voicing," J. Acoust. Soc. Am. **53**(6), 1632–1645 (1972).